analytical chemistry

Article

pubs.acs.org/ac

Assay of Genome-Wide Transcriptome and Secreted Proteins on the Same Single Immune Cells by Microfluidics and RNA Sequencing

Justin George[†] and Jun Wang*[,†,‡]

[†]Multiplex Biotechnology Laboratory, Department of Chemistry, University at Albany, State University of New York, Albany, New York 12222, United States

[‡]Cancer Research Center, University at Albany, State University of New York, Rensselaer, New York 12144, United States

Supporting Information

ABSTRACT: Given vast heterogeneity of immune cells, searching for gene expression and transcriptional networks belonging to specific cellular functions such as cytokine production has been challenging. To overcome this limitation, we developed a splittable single-cell microchip that integrates a high-density antibody array for cytokine protein detection, while the same single cells with protein profile can be subsequently sequenced to obtain the genome-wide transcriptome. Combined with bioinformatics algorithms, we discovered a subgroup of highly coexpressed genes correlating with TNFα secretion in mouse macrophage cells. This technology and the data analysis may lead to an unprecedented understanding of regulation mechanisms of the immune system and have the potential to impact disease treatment and drug discovery.

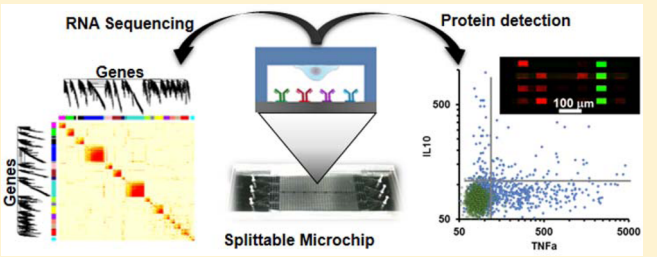

Individual cells are always heterogeneous in gene expression, which leads to diverse phenotypes and functions such as those in immune responses to infection and cancer progression.[1,2] Cytokines that are secreted mainly by immune cells play a critical role in inflammation and chronic disease development.[3−5] The ability of measuring genes and the related transcriptional network responsible for cytokine protein production, if available, would be valuable for better understanding, and even controlling, immune responses. Indeed, the central dogma involving mRNA and proteins at the single-level has not been systemically studied due to technical difficulty.

There are a few technologies available for separately assaying cytokines or gene expression in single cells. However, measurement of both gene expression and proteins representing certain phenotypes/functions has only been recently emerging. The single-cell assays by mass cytometry or multiparameter flow cytometry are high-throughput, high-content functional proteomic technologies that are capable of characterizing cells by surface markers and intracellular signaling proteins, and thus are superior to Elispot for quantitating the amount of functional proteins in single cells.[6,7] However, blocking protein secretion by those methods will inevitably introduce a nontrivial perturbation to signaling networks. Microfluidics such as microengraving microchip and single-cell barcode chip are the major technologies for multiplexed single-cell cytokine detection.[8−12] Both are sensitive enough to measure cytokines below 100 copies per cell. But they are rarely used to detect both cytokines and gene expression from the same single cells. Recently, mass cytometry has been combined with proximity ligation assay to measure about 40 different mRNA and proteins from the same single cells.[13] Another convenient technique based on droplet digital PCR and proximity ligation assay has quantitated 3 proteins and their genes from single cells with lower-end facilities.[14] These technologies, together with others based on barcode chip and fluorescence in situ hybridization,[15−18] are limited by the number of detected mRNAs and are thus not discovery tools to find a cohort of genes responsible for protein production. Single-cell RNA sequencing is able to survey the whole transcriptome from statistical number of cells to globally seek for genes of interest.[19] But none of RNA-seq related technologies allows for simultaneous detection of both proteins and transcripts.

Here we present a method to address these limitations by measuring both genome-wide transcriptome and secreted cytokine proteins from the same single cells. Mouse macrophage cells stimulated with lipopolysaccharide (LPS) were used to demonstrate the ability of our technology for assaying a few cytokines and the gene expression associated with inflammatory immune response. The correlations of individual proteins and their transcripts are varied significantly, while highly secreted cytokines tend to be more consistent with their gene expression. Enabled by weighted gene coexpression network analysis (WGCNA),[20] we discovered the transcriptional networks related to TNFα production and regulation. Our technology is the first of the similar kind that permits genome-

Received: August 16, 2016
Accepted: September 14, 2016

DOI: 10.1021/acs.analchem.6b03214
Anal. Chem. XXXX, XXX, XXX−XXX

wide surveying of gene expression related with cellular functions, and is able to provide deeper insights into complex regulation of heterogeneous cell populations.

EXPERIMENTAL SECTION

Microchip Fabrication. The general procedures for fabricating the splittable microchip by lithography were described previously.[21,22] Briefly, a multilayer mold was constructed by patterning SU-8 (Microchem) photoresists on a 4″ silicon wafer. The first layer serves as the base for all the following 2 layers, and contains circular holes with ∼100 μm depth which was converted to posts after polydimethylsiloxane (PDMS; Ellsworth Adhesives) casting. After development, the second layer for formation of microchambers was fabricated using SU-8 2015 (thickness of 25 μm). The final SU-8 2025 layer (thickness of 50 μm) formed the mold for the microchannels in a grid design with inverted "bowl" features at the intersections of the gridlines. The bowls have hollow centers that are aligned with the circular holes of the first layer, so that the PDMS posts carved out of the mold attain a height of 150 μm. The features of the second and third layer were aligned to ensure that the microchambers were enclosed in the microchannel grids. The features of the mold were transferred to PDMS with 10:1 ratio of base to curing agent. The PDMS replica was finally mated with an antibody array to become a functional microchip. The resulting microchip had a fixed height of 75 mm, containing ∼6000 microchambers 1000 μm × 30 μm × 25 μm for single cell isolation.

Antibody Array Fabrication. The procedure of preparing the antibody barcode array on a glass substrate can be found in our previous publication.[23] A PDMS mold was fabricated first using standard soft lithography techniques, and was then attached to a poly-L-lysine slide (Thermo Scientific) to form long and narrow microchannels by baking at 80 °C for 2 h. Six types of amine-modified oligonucleotides (labeled as D, E, F, G, H, and I) were flowed into individual microchannels and patterned on the glass slide surface through bis (sulfosuccinimidyl) suberate (BS3; Thermo Scientific) cross-linking. The array was validated to ensure no crosstalk. This oligonucleotide array was converted into an antibody array by incubating the cocktail of antibody-oligonucleotide conjugates at 2.5 μg/mL on the slide at 37 °C. These antibodies were chosen to target TNFα, IL6, IL10, GM-CSF, and IFNγ and were tagged with complementary oligonucleotides (D′, E′, F′, G′, and I′).[23] Conversion was always done immediately preceding on-chip protein detection assays. The arrays were validated and calibrated by detecting recombinant proteins at concentrations of 10 to 10^4 pg/mL.

Cell Sample Preparation. Mouse macrophages were derived from monocytes collected from BALB/c mouse bone marrow using a 23-gauge needle.[24] Cells were cultured for 5−7 days at the beginning in the macrophage differentiation medium (DMEM/F12−10 medium with 100 U/mL M-CSF, 10% FBS, 100 U/mL penicillin G, and 100 μg/mL streptomycin) at 37 °C in 5% CO_2 incubator. As a uniform monolayer of macrophage was formed, cells were ready for further analysis. A mild condition using 1 mM EDTA was used to detach cells, followed by resuspension in phosphate buffered saline (PBS) at a concentration of 0.5 × 10^6 cells/ml for on-chip experiments. Cells were optionally purified by CD11b microbeads (Miltenyi Biotec), and over 90% cells were recovered, showing that most cells were $CD11b^+$. Raw 264.7 cells (ATCC) were also used for optimizing the microchip operation. These cells were cultured in the complete medium (DMEM/F12−10 medium supplemented with 10% FBS, 100 U/mL penicillin G, and 100 μg/mL streptomycin).

To stimulate macrophages, 100 ng/mL lipopolysaccharide (LPS, Sigma) was added to the complete medium, and cells were cultured in this medium at 37 °C in 5% CO_2 incubator. Calcein AM (0.2 μM, Life Technologies) was added to the culture medium to distinguish live cells and facilitate cell counting. One-cell chambers are distinguished from zero-cell chambers by imaging.

Microchip Single-Cell Secretion Analysis. The PDMS surface was oxidized by plasma cleaner (Harrick Plasma) for 1 min and coated with 100 μg/mL collagen (Corning). Macrophage cells at a concentration of 0.5 × 10^6 cells/mL in PBS were deposited on the flipped PDMS surface which contains features for microchannels and microchambers. After incubation at 37 °C for 10 min, the unbound cells were washed off by complete medium, and an antibody array glass slide was placed on the top and was assembled with the PDMS. The whole microchip was mounted on a clamp, which permits adjustment of mechanical pressure onto the microchip to seal the microchambers containing single cells. The microchip was subsequently incubated at 37 °C in a 5% CO_2 incubator for 6 h. After incubation and labeling microchannels, the PDMS part was carefully separated from the antibody array slide, in order to retain cells in microchambers. The PDMS slab carrying cells in the microchambers (slots) was immediately transferred to a 4 °C refrigerator. Biotinylated detection antibodies and streptavidin-Alexa 647 (Life Technologies) were sequentially added to the glass slide to complete sandwich ELISA steps. After data collection using GenePix scanner (Molecular Devices), the addresses of microchambers with the secretion profile of interest were indexed, and the corresponding addresses on the PDMS slab were found. A homemade stage was built to stabilize a syringe connected with a needle (Hamilton; 32 gauge), which was used to pick up single cells in 1% triton-X100 and transfer them to a 96 well plate at 4 °C.

Single-cell data were digitized by GenePix Pro (Molecular Devices) and processed by Prism (GraphPad) and Matlab (Mathworks) for comparison of 0 cell data vs 1 cell data. Unpaired, two-tailed t test was used to determine statistically significant differences. A P value less than 0.05 is considered statistically significant and is denoted with *, while ** and *** represent $P < 0.01$ and $P < 0.001$, respectively. Error bars on scatter dot plots represent the interquartile range of the sample, whereas red bars denote the median intensity. Hierarchical clustering was applied to single-cell data above the threshold set for background fluorescence (mean + standard deviation of zero-cell fluorescence). Cluster 3.0 (Stanford University) with TreeView 3.0 (Java) were used to generate heat maps. Data was normalized by median-centering then hierarchical clustering was performed using a correlation similarity metric with centroid linkage clustering algorithm.

RNA Sequencing. The process of cDNA synthesis and amplification from single cells follows the protocol of SMART-Seq2 Ultra Low Input RNA kit (Clontech Laboratories). The first strand cDNA synthesis from lysed cells was primed by the 3′ SMART-Seq CDS Primer II A and the oligonucleotides for template switching at the 5′ end of the transcripts. The reversed transcribed cDNA was amplified for 28 cycles due to ultralow starting mRNA amount. For bulk samples, cDNA was obtained using SuperScript III CellsDirect cDNA Synthesis Kit (Life Technologies). The ∼1000 cells were lysed and treated with

DOI: 10.1021/acs.analchem.6b03214
Anal. Chem. XXXX, XXX, XXX−XXX

DNase I to remove genomic DNA. The 10 μM Oligo $(dT)_{20}$ and 0.5 mM dNTPs were added to the samples first, incubated for 5 min at 70 °C, and then 10 U of SuperScript reverse transcriptase was applied to synthesize the cDNA at 50 °C for 50 min. The same condition was repeated 3 times.

Amplified cDNA was purified by Agencourt AMPure XP beads, and was further quantified by Nanodrop 2000 and validated by Agilent 2100 Bioanalyzer and High Sensitivity DNA kit (Agilent). The yield above ~0.5 ng cDNA was acceptable for further library preparation using Nextera XT DNA Library Preparation Kit and Nextera XT Index Kit (Illumina). The advantage of this library preparation system is that it can efficiently work with low cDNA samples. Following the kit protocol, ~200 pg cDNA from each sample were tagmentated at 55 °C for 5 min with transposase. The tagmented DNAs were further added with index adaptors, and were amplified by PCR for 10 cycles before purification by AMPure XP beads. DNA libraries were sequenced on the Illumina HiSeq2000, and single-end reads of 100 bp length were obtained.

After removing adapter sequences, reads were mapped and aligned to UCSC mouse mm9 genome with two mismatches, two gaps and one multihit allowed, using TopHat 2.1.0 and Bowtie 1.1.1 by reading 35 bp. Counts per million (CPM) were estimated by htseq-count function in HTSeq Python package and were normalized by edgeR function.[25] Any genes with totally ≤5 CPM in all single cell samples were removed, which resulted in 4891 genes remained in the list for further analysis.

Transcriptomic Coexpression Network Analysis. Weighted gene coexpression network analysis (WGCNA) in R script was used to construct genome-wide transcriptional network for the macrophage cells. WGCNA not only identifies coexpressed genes according to their correlation, but also relates a subgroup of genes with external properties. First, a correlation matrix among all pairs of genes was created using "signed" coexpression measure with power 12, which is the interpreted as a soft-threshold of the correlation matrix. A topological overlap was calculated based on the resulting adjacency matrix. Genes with highly similar coexpression relationship were grouped and hierarchically clustered. A dynamic hybrid tree cut algorithm was adopted to cut the hierarchal clustering tree, and thereafter to define modules visualized as tree branches. Thus, every module was a cluster of highly correlated genes, and was assigned different colors. Within a module, the correlations were above 0.7. The genes with the highest value of module membership were considered to be intramodular hub genes. The hub genes represent the expression profiles of the entire module.

The first principal component of each module was used to correlate with the external property, here in cytokine secretion level, to search for related genes responsible for cytokine production. The Pearson's correlation coefficients were calculated along with P values. $P < 0.05$ was deemed as the study-wide empirical threshold. The chord diagram was generated by a Matlab program, and the dendrogram of gene correlation clustering was superimposed on the chord diagram.

Gene Ontology Pathway Enrichment Analysis. To identify common functional categories represented by GO and curated gene sets, the Molecular Signatures Database (MsigDB; http://software.broadinstitute.org/gsea/index.jsp) was used to compute the overlaps with the gene list in selected modules. We present the enrichment of each module in pathways with significance P value < 10^{-10} and false discovery rate (FDR) q value < 10^{-8}.

Microscopy Imaging. Images of the chip and cells after staining were taken systematically on an inverted fluorescence microscope (Olympus IX73) equipped with three fluorescent filter sets: a green fluorescein filter set (U-FF, Olympus; excitation filter 450−490 nm, dichroic 500 nm long pass, emission 520 nm long pass), a yellow Cy3 filter set (U-FF, Olympus; excitation filter 528−553 nm dichroic 565 nm long pass, emission 590−650 nm), and a red Cy5 filter set (U-FF, Olympus; excitation filter 590−650 nm, dichroic 660 nm long pass, emission 665−740 nm). A microscope objective (UPlanApo, Olympus, 4X/0.16; UPlanFLN, Olympus, 10X/0.30/Ph1; UCPlanFLN, Olympus, 20X/0.70/Ph2) was used to collect fluorescence light. A digital camera (Zyla sCMOS, Andor) mounted on the microscope was used to capture images using Andor SOLIS software.

Determination of Limit of Detection. The limit of detection (LOD) was calculated using a previously reported method.[26] The limit of blank (LOB) was calculated first from the mean ($mean_{blank}$) and standard deviation (SD_{blank}) of the fluorescence signals of blank microarray using the equation LOB = $mean_{blank}$ + 1.645 (SD_{blank}). The LOD was then calculated by incrementing the LOB with the standard deviation of fluorescence signals (SD_{lc}) obtained from 10 to 10^4 pg/mL of recombinant proteins, using the equation LOD = LOB + 1.645 (SD_{lc}).

RESULTS AND CONCLUSIONS

The general procedure of measuring a few cytokines and the genome-wide transcriptome is shown in Figure 1. Single cells are seeded into nanosize microchambers of the splittable

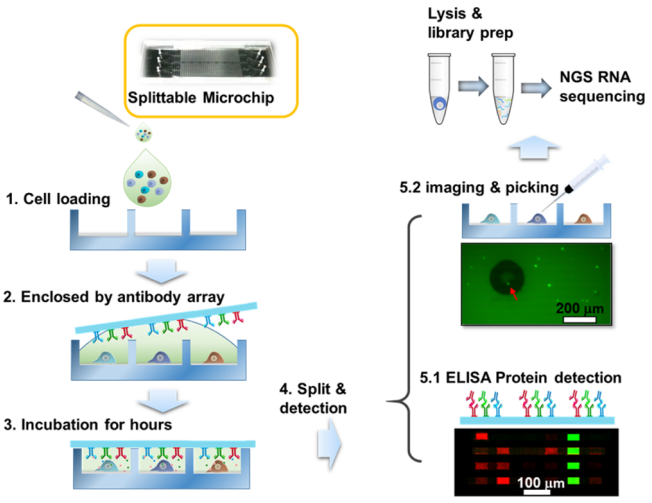

Figure 1. Scheme of detecting both secreted proteins and transcriptome from the same single cells. The PDMS part of the microchip is coated with collagen and is seeded with single cells. Subsequently, the microchambers are sealed with an antibody array for capturing secreted cytokines. Then the microchip is split for ELISA protein detection and cell imaging separately. Single cells with a protein profile are picked up by a 32G syringe and lysed immediately for next generation sequencing (NGS) of mRNAs. The image in step 5.1 is a typical result after detection, with each row corresponding to a single cell microchamber. Detected proteins are in red color and the reference is in green color. The arrow in step 5.2 indicates a fluorescent cell captured by the syringe needle.

DOI: 10.1021/acs.analchem.6b03214
Anal. Chem. XXXX, XXX, XXX−XXX

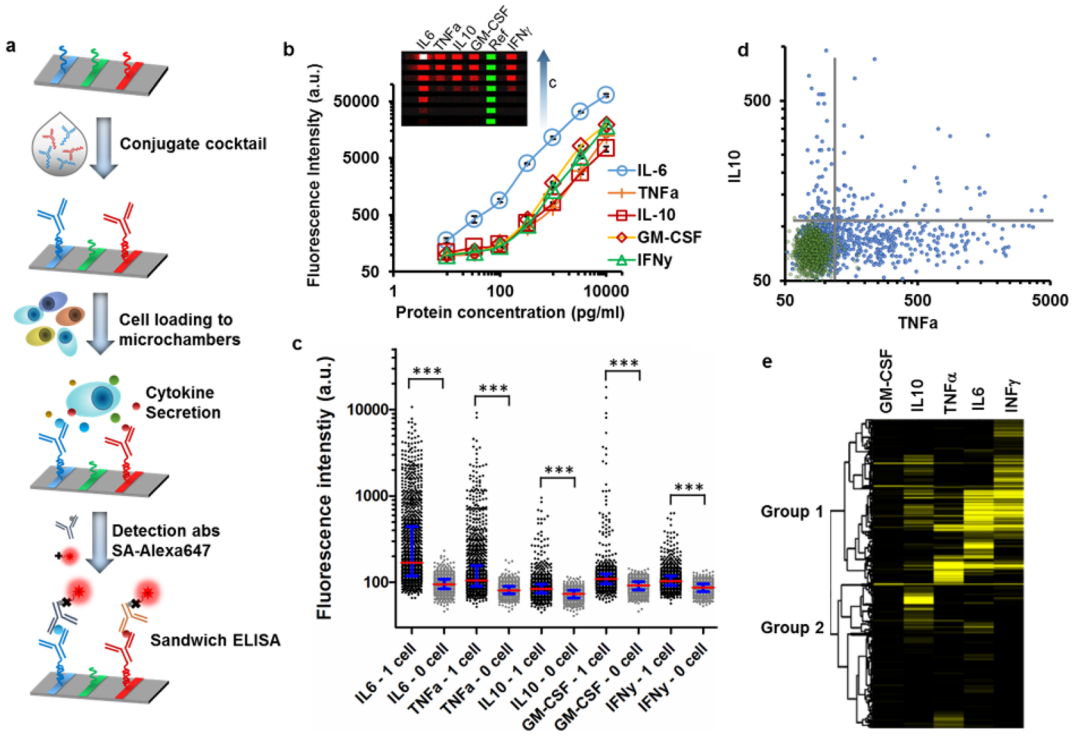

Figure 2. (a) Experimental procedure of multiplexed cytokine detection based on sandwich ELISA. (b) Calibration curves for immunoassays performed on-chip using recombinant protein IL6, TNFα, GM-CSF, IL10, and IFNγ. Error bars denote standard deviation from the mean of 3 repeats. Inset: Fluorescence readouts obtained for different concentrations of recombinant protein used in calibration. (c) Dot plot showing fluorescence data for secreted cytokines from one-cell experiments in the microchip compared to background levels from zero-cell experiments. *P* values are 0.05 (*), 0.01 (**), and 0.001 (***), with 0.05 considered statistically significant. Red bars are median values, and blue bars are interquartile ranges. (d) Scatter dot plot of TNFα and IL10 produced by single cell (blue) and in empty microchambers (green). (e) Heatmap comparing relative levels of five cytokines from single cells. Unsupervised clustering based on correlation matrices and centroid linkage is used to group single cells (rows).

microchip first and attach to the surface. A glass slide carrying a high-density, multiplexed antibody array is placed on the PDMS to seal the microchambers and isolate single cells. After incubation for hours, cytokines secreted by the individual cells are captured by the antibody array. Then the PDMS slab is separated from the glass slide, and the addresses of single cells are imaged while their secretion profiles are detected by sandwich ELISA. The single cells with interesting secretion profiles are picked up by an ultrafine needle syringe, and are immediately lysed in 1% triton X-100 solution. Following RNA sequencing protocols, cDNA is synthesized first from mRNA and is amplified before library preparation. After sequencing, reads are mapped and aligned to find the corresponding genes. Then WGCNA is applied to generate genome-wide transcriptomic network using the single-cell RNA sequencing results. We also employ WGCNA to relate the sub groups of transcriptome to the cytokine secretion profiles of single cells, and to discover the transcriptional network pertinent to immunologically competent single cells.

The splittable single-cell microchip is designed in the way that the PDMS replica and the glass slide are attached to each other only by external mechanical force. The details of other auxiliary features including a large-scale microchannel grid and posts can be found in our previous publications.[21−23] Those features support fluidic flow within the entire microchip and segmentation of all cell microchambers. The whole microchip in this study has 6720 microchambers (distributed in 15 × 28 grids, and each grid hosts 16 microchambers). All the microchambers are addressable; for example, a selected location could be column2−row15−line10. This gives us enormous convenience to match the single cells in microchambers with the corresponding protein secretion profiles after splitting the microchip. Each microchamber is only 1000 μm × 30 μm × 25 μm, or 0.75 nL, for single cell isolation and incubation, which promises high sensitivity when detecting limited number of cytokines secreted by macrophage. We work with macrophage cells not only because they produce a large quantity of cytokines once challenged by lipopolysaccharide (LPS), but also because they adhere to the microchamber surface so that they remain in the same location and are thus trackable after the microchip is split. A total of 87% macrophage cells were retained if the microchambers were coated with collagen and cells were adherent during the 6 h incubation time. Without coating, cells appeared in spherical shape, indicating no attachment, and >90% cells were lost after splitting the microchip.

Five cytokines studied on our platform include interleukin 6 (IL6), tumor necrosis factor α (TNFα), granulocyte-macrophage colony-stimulating factor (GM-CSF), interleukin 10 (IL10), and interferon gamma (IFNγ). The proinflammatory cytokine TNFα and IL6 are commonly produced after TLR activation via LPS stimulation, while the anti-inflammatory cytokine IL10 could be generated simultaneously.[27,28] The other two cytokines, GM-CSF and IFNγ, are also closely related with monocyte differentiation and adaptive immune system's response to infection.[29,30] The procedure of cytokine protein detection is shown in Figure 2a. The laboratory-developed microarray was fabricated as an oligonucleotide array

DOI: 10.1021/acs.analchem.6b03214
Anal. Chem. XXXX, XXX, XXX−XXX

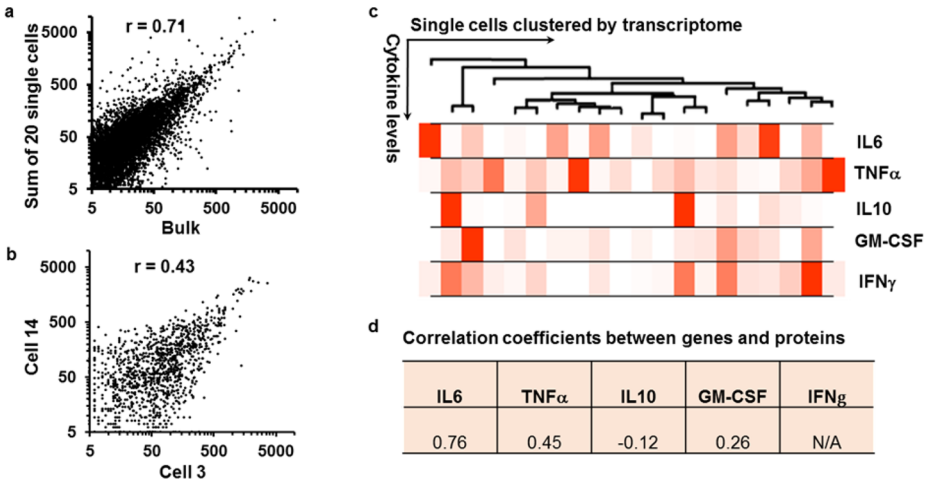

Figure 3. RNA sequencing of single macrophage cells with cytokine secretion profiles. (a) Correlation of transcript expression levels between a ~1000 cell population and the sum of 20 single cells. (b) Dot plot of two randomly selected cell 3 and cell 14. (c) Clustering of 20 single cells according to the dissimilarity of their transcriptomic profiles by "average" agglomeration method in R packages. The heatmap below denotes relative secretion levels of cytokines for each single cell. (d) Correlation coefficients of cytokine proteins and their corresponding transcripts. NA means not applicable.

first using flow patterning technique. Six single-stranded DNAs that are orthogonal to each other were carefully selected and validated (Table S1), each of which were flowed into a separate microchannel of a microchip with a total of 10 or 20 microchannels in parallel winding from one end to the other end (Figure S1). The oligonucleotide array was converted into an antibody array using antibody-ssDNA conjugates, since the ssDNA on each antibody only binds to its complementary ssDNA on the array. Using commercial ssDNA array with the same ssDNA sequences, we confirmed no crosstalk of our reagents (Figure S2). After the array slide was mated with the PDMS replica for single cell measurement, we examined the sensitivity of the single cell chip for protein quantification. The detection limit for five cytokines IL6, TNFα, GM-CSF, IL10, and IFNγ are 3.7, 69, 84, 96, and 73 pg/mL, respectively. Except IL6, the detection limits are slightly higher than those based on well plates (Figure 2b). This might be because the small volume of microchambers limited the access of the antibody array to recombinant proteins.

We used the single cell microchip to measure cytokine secretion profiles of single macrophage cells derived from monocytes in mouse bone marrow. Cells were stimulated by 100 ng/mL LPS and incubated in microchambers for 6 h (Figure S3). We set 6 h as the incubation time because the major inflammatory factors TNFα and IL6 could be secreted to a detectable level, while the transcriptome at the activated state might not be fundamentally changed.[31,32] At the bulk level, those two cytokines can be produced above 1 ng/mL with 6 h incubation time. The significantly longer incubation time may miss the time window of obtaining the transcription directly relevant to cytokine production. Figure 2c shows the secretion levels of five cytokines detected from microchambers with one cell and zero cell, where single cells produce significant amount of cytokines. Just like flow cytometry, we also set a threshold for each protein for clustering purpose. The cytokine level above the threshold set for background fluorescence (mean + standard deviation of zero-cell fluorescence) is regarded as a positive event. From these single-cell data, we quantified 62% single macrophage cells significantly secreting TNFα and 8% those cells produce >1 ng/mL TNFα, while 23% cells significantly secrete IL10. Thus, within 6 h stimulation time, cells are already highly activated and produce proteins to extracellular environment, which is consistent with the previous reports.[32,33] Interestingly, TNFα and IL10 show anticorrelation in the dot plot (Figure 2d). Unsupervised clustering of all single cells according to their cytokine secretion profiles also result in two large groups, dominated by TNFα, IL6 and IFNγ in group 1 and IL10 in group 2. This phenomenon may be caused by the opposite role of TNFα and IL10 in both innate and specific immune responses.[34,35] While LPS stimulated macrophage cells are normally present in M1 type, the TLR activation may elicit IL-10 as well in another subtype.[36,37]

The microchip was split into a PDMS replica carrying cells and an array slide bearing antibody array, after incubation of single cells on the microchip for 6 h. ELISA detection was separately completed on the array slide, and single cells were matched with cytokine profiles before being carefully picked up by a 32 G syringe needle for RNA extraction and sequencing. We used Clontech SMART-Seq2 method to reverse transcribe mRNA to cDNA and constructed library with Nextera kits from Illumina (SI, Method). After quality control, 23 out of 90 single cells were sequenced with 10 million single end reads, and three cells were screened out due to low reads. After removing adapter sequences, reads were mapped and aligned to UCSC mouse mm9 genome with two mismatches, two gaps, and one multihit allowed. Genes with counts per million (CPM) ≤ 5 were discarded, resulting in 4891 genes left for network analysis. Substantial heterogeneity in gene expression has been found between single cells. Figure 3a shows the correlation (r = 0.71) of the transcriptome profile of 1000 cells compared with that of the sum of 20 single cells. The correlation coefficients drop significantly to 0.43 when two individual cells are compared (Figure 3b). All 20 cells were clustered together by transcriptome profile, and their cytokine production was normalized and placed together in Figure 3c. Various correlation coefficients between transcripts and cytokines are found (Figures 3d and S4). IL6 and TNFα are highly secreted proteins and show certain degree of correlation (r = 0.76 with P value = 0.000072 and r = 0.45 with P value = 0.043), whereas other cytokines with low secretion levels may not be correlated

DOI: 10.1021/acs.analchem.6b03214
Anal. Chem. XXXX, XXX, XXX−XXX

with their gene expression (P value > 0.05). The correlation maps of proteins and transcriptome also show that they exhibit cellular heterogeneity in different ways (Figure S5). Although only 20 single cells are profiled, this cell sample size can be sufficient to extract key transcription information from the high-content, genome-wide sequencing results, demonstrated in other single-cell RNA sequencing reports.[19,20]

Next we asked what transcriptional networks are related to the cytokine production. Based on single-cell RNA-seq data, the whole transcriptome network was constructed using WGCNA (Figures 4a and S6) to obtain multiple gene-network modules

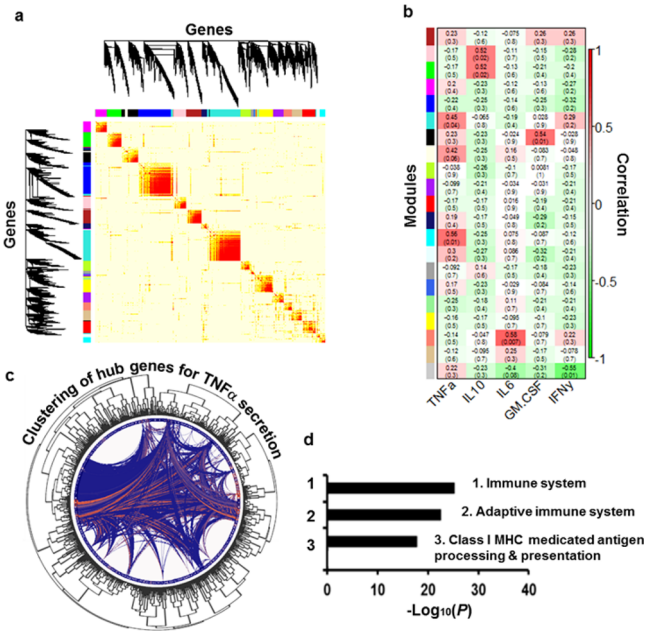

Figure 4. Weighted transcriptional network analysis identifies genes related to cytokine protein production. (a) Genome-wide whole transcriptional network visualized by heatmap. Dark color represents high topological overlap matrix (TOM), and light color represents low TOM. The gene dendrogram and modules in various colors are along the left side and the top. (b) Cytokine protein association of each module (left), represented by each module's first principal component (eigengene). The numbers in each unit are correlation coefficient between protein expression and eigengene as well as the corresponding P value, where $P < 0.05$ is regarded as significance. The correlation coefficients are shown as heatmap where red color and green color in the heatmap indicate high association and low association, respectively. (c) Chord diagram of hub genes within the cyan module that is highly correlated with TNFα secretion. Blue color and red color of chords denotes relatively lower topological overlap and higher topological overlap. The outlayer dendrogram is hierarchical clustering of genes within the cyan module. (d) GO pathway enrichment analysis of the cyan module reveals that genes in this module are highly related to immune response (Table S2).

(shown in different colors). Genes in the dendrogram are hierarchically clustered according to their topological overlap. To identify which module is related to individual cytokine secretion, module eigengene (i.e., the first principal component of a give module) that represents the gene expression profile of a module was calculated first and was then correlated with cytokine levels of the same single cells. The correlation coefficients and the P values are shown in Figure 4b. We identified the cyan module highly correlated with TNFα secretion. The connectivity >0.5 between the genes in the cyan module extracted from WGCNA is plotted in Figure 4c, while all the genes in this module are clustered to visualize hub genes (i.e., highly connected genes within a module; colored cords in Figure 4c; Figure S7). These hub genes may contain the key regulatory network for TNFα production. We employed the gene ontology (GO) pathway enrichment analysis using Molecular Signatures Database (MsigDB; Broad Institute) on all the genes in the cyan module. This module contains many immune related genes including, for example, TNF receptor associated factor 2 (TRAF2) and its inhibitor F-box only protein 3 (FBXO3).[38] Suppressor of cytokine signaling 3 (SOCS3) is also present which regulates TNFα indued inflammatory response.[39] Thus, while large quantity of cytokines is produced and the pathways like MAPK that was also detected are involved, the production is well controlled through complicated regulatory networks.

CONCLUSIONS

In summary, we have measured both transcriptome and cytokine proteins from the same single macrophage cells, and have demonstrated how to exploit the single-cell transcriptome information to find gene expression and network pertinent to the cytokine-secreting cell subtype. It is found that the proinflammatory factor TNFα and the anti-inflammatory factor IL10 are secreted by different cell types after LPS stimulation. Through WGCNA, we have discovered an eigengene that might exquisitely regulate TNFα production. Our method should be applicable for other adherent cell types. For nonadherent cells, they could also be analyzed by our method as long as they could be retained through interaction between surface receptors and antibodies in the microchambers after splitting.[33] Although the throughput of the current technology is limited, with fast advancement and lower cost of RNA sequencing technology, our integrated technology can find broader applications in immunology and other biomedical fields. This discovery tool may facilitate deeper understanding of cellular machinery, improve disease treatment and accelerate drug discovery in the future.

ASSOCIATED CONTENT

Supporting Information

The Supporting Information is available free of charge on the ACS Publications website at DOI: 10.1021/acs.analchem.6b03214.

Supporting figures and tables (PDF).

AUTHOR INFORMATION

Corresponding Author

*E-mail: jwang34@albany.edu.

Notes

The authors declare no competing financial interest.

ACKNOWLEDGMENTS

This work was supported by the Presidential Initiatives Fund for Research and Scholarship and the startup fund from SUNY Albany to J.W.

REFERENCES

(1) Lin, Y. H.; Elowitz, M. B. *Mol. Cell* **2016**, *61*, 791−792.
(2) Ma, C.; Fan, R.; Ahmad, H.; Shi, Q.; Comin-Anduix, B.; Chodon, T.; Koya, R. C.; Liu, C. C.; Kwong, G. A.; Radu, C. G.; Ribas, A.; Heath, J. R. *Nat. Med.* **2011**, *17*, 738−743.

DOI: 10.1021/acs.analchem.6b03214
Anal. Chem. XXXX, XXX, XXX−XXX

(3) O'Shea, J. J.; Ma, A.; Lipsky, P. *Nat. Rev. Immunol.* **2002**, *2*, 37−45.
(4) Dranoff, G. *Nat. Rev. Cancer* **2004**, *4*, 11−22.
(5) Vilcek, J.; Feldmann, M. *Trends Pharmacol. Sci.* **2004**, *25*, 201−209.
(6) Perfetto, S. P.; Chattopadhyay, P. K.; Roederer, M. *Nat. Rev. Immunol.* **2004**, *4*, 648−U645.
(7) Bendall, S. C.; Simonds, E. F.; Qiu, P.; Amir, E. A. D.; Krutzik, P. O.; Finck, R.; Bruggner, R. V.; Melamed, R.; Trejo, A.; Ornatsky, O. I.; Balderas, R. S.; Plevritis, S. K.; Sachs, K.; Pe'er, D.; Tanner, S. D.; Nolan, G. P. *Science* **2011**, *332*, 687−696.
(8) Varadarajan, N.; Julg, B.; Yamanaka, Y. J.; Chen, H. B.; Ogunniyi, A. O.; McAndrew, E.; Porter, L. C.; Piechocka-Trocha, A.; Hill, B. J.; Douek, D. C.; Pereyra, F.; Walker, B. D.; Love, J. C. *J. Clin. Invest.* **2011**, *121*, 4322−4331.
(9) Gong, Y. A.; Ogunniyi, A. O.; Love, J. C. *Lab Chip* **2010**, *10*, 2334−2337.
(10) Shi, Q. H.; Qin, L. D.; Wei, W.; Geng, F.; Fan, R.; Shin, Y. S.; Guo, D. L.; Hood, L.; Mischel, P. S.; Heath, J. R. *Proc. Natl. Acad. Sci. U. S. A.* **2012**, *109*, 419−424.
(11) Ma, C.; Cheung, A. F.; Chodon, T.; Koya, R. C.; Wu, Z. Q.; Ng, C.; Avramis, E.; Cochran, A. J.; Witte, O. N.; Baltimore, D.; Chmielowski, B.; Economou, J. S.; Comin-Anduix, B.; Ribas, A.; Heath, J. R. *Cancer Discovery* **2013**, *3*, 418−429.
(12) Son, K. J.; Rahimian, A.; Shin, D. S.; Siltanen, C.; Patel, T.; Revzin, A. *Analyst* **2016**, *141*, 679−688.
(13) Frei, A. P.; Bava, F. A.; Zunder, E. R.; Hsieh, E. W. Y.; Chen, S. Y.; Nolan, G. P.; Gherardini, P. F. *Nat. Methods* **2016**, *13*, 269.
(14) Albayrak, C.; Jordi, C. A.; Zechner, C.; Lin, J.; Bichsel, C. A.; Khammash, M.; Tay, S. *Mol. Cell* **2016**, *61*, 914−924.
(15) de Planell-Saguer, M.; Rodicio, M. C.; Mourelatos, Z. *Nat. Protoc.* **2010**, *5*, 1061−1073.
(16) Zhang, Y.; Tang, Y.; Sun, S.; Wang, Z.; Wu, W.; Zhao, X.; Czajkowsky, D. M.; Li, Y.; Tian, J.; Xu, L.; Wei, W.; Deng, Y.; Shi, Q. *Anal. Chem.* **2015**, *87*, 9761−9768.
(17) Kochan, J.; Wawro, M.; Kasza, A. *BioTechniques* **2015**, *59*, 209−221.
(18) Wu, B.; Buxbaum, A. R.; Katz, Z. B.; Yoon, Y. J.; Singer, R. H. *Cell* **2015**, *162*, 211−220.
(19) Shalek, A. K.; Satija, R.; Adiconis, X.; Gertner, R. S.; Gaublomme, J. T.; Raychowdhury, R.; Schwartz, S.; Yosef, N.; Malboeuf, C.; Lu, D.; Trombetta, J. J.; Gennert, D.; Gnirke, A.; Goren, A.; Hacohen, N.; Levin, J. Z.; Park, H.; Regev, A. *Nature* **2013**, *498*, 236−240.
(20) Xue, Z.; Huang, K.; Cai, C.; Cai, L.; Jiang, C. Y.; Feng, Y.; Liu, Z.; Zeng, Q.; Cheng, L.; Sun, Y. E.; Liu, J. Y.; Horvath, S.; Fan, G. *Nature* **2013**, *500*, 593−597.
(21) Wang, J.; Tham, D.; Wei, W.; Shin, Y. S.; Ma, C.; Ahmad, H.; Shi, Q.; Yu, J.; Levine, R. D.; Heath, J. R. *Nano Lett.* **2012**, *12*, 6101−6106.
(22) Kravchenko-Balasha, N.; Wang, J.; Remacle, F.; Levine, R. D.; Heath, J. R. *Proc. Natl. Acad. Sci. U. S. A.* **2014**, *111*, 6521−6526.
(23) Ramirez, L. S.; Wang, J. *J. Visualized Exp.* **2016**, *107*, e53644.
(24) Zhang, X.; Goncalves, R.; Mosser, D. M. *Current Protocols in Immunology*; Coligan, J. E., Ed.; John Wiley and Sons, 2008; Chapter 14, Unit 14 11, DOI: 10.1002/0471142735.im1401s83.
(25) Anders, S.; McCarthy, D. J.; Chen, Y. S.; Okoniewski, M.; Smyth, G. K.; Huber, W.; Robinson, M. D. *Nat. Protoc.* **2013**, *8*, 1765−1786.
(26) Armbruster, D. A.; Pry, T. *Clin. Biochem. Rev.* **2008**, *29*, S49−S52.
(27) Murray, P. J. *Proc. Natl. Acad. Sci. U. S. A.* **2005**, *102*, 8686−8691.
(28) Couper, K. N.; Blount, D. G.; Riley, E. M. *J. Immunol.* **2008**, *180*, 5771−5777.
(29) Lehtonen, A.; Matikainen, S.; Miettinen, M.; Julkunen, I. *J. Leukocyte Biol.* **2002**, *71*, 511−519.
(30) Delneste, Y.; Charbonnier, P.; Herbault, N.; Magistrelli, G.; Caron, G.; Bonnefoy, J. Y.; Jeannin, P. *Blood* **2003**, *101*, 143−150.
(31) Kirkley, J. E.; Thompson, B. J.; Coon, J. S. *Scand. J. Immunol.* **2003**, *58*, 51−58.
(32) Bjorkbacka, H.; Fitzgerald, K. A.; Huet, F.; Li, X.; Gregory, J. A.; Lee, M. A.; Ordija, C. M.; Dowley, N. E.; Golenbock, D. T.; Freeman, M. W. *Physiol. Genomics* **2004**, *19*, 319−330.
(33) Han, Q.; Bagheri, N.; Bradshaw, E. M.; Hafler, D. A.; Lauffenburger, D. A.; Love, J. C. *Proc. Natl. Acad. Sci. U. S. A.* **2012**, *109*, 1607−1612.
(34) Rojas, M.; Olivier, M.; Gros, P.; Barrera, L. F.; Garcia, L. F. *J. Immunol.* **1999**, *162*, 6122−6131.
(35) Ismail, N.; Stevenson, H. L.; Walker, D. H. *Infect. Immun.* **2006**, *74*, 1846−1856.
(36) Martinez, F. O.; Gordon, S. *F1000Prime Rep.* **2014**, *6*, 13.
(37) Franchimont, D.; Martens, H.; Hagelstein, M. T.; Louis, E.; Dewe, W.; Chrousos, G. P.; Belaiche, J.; Geenen, V. *J. Clin. Endocrinol. Metab.* **1999**, *84*, 2834−2839.
(38) Mallampalli, R. K.; Coon, T. A.; Glasser, J. R.; Wang, C.; Dunn, S. R.; Weathington, N. M.; Zhao, J.; Zou, C. B.; Zhao, Y. T.; Chen, B. B. *J. Immunol.* **2013**, *191*, 5247−5255.
(39) Ehlting, C.; Lai, W. S.; Schaper, F.; Brenndorfer, E. D.; Matthes, R. J.; Heinrich, P. C.; Ludwig, S.; Blackshear, P. J.; Gaestel, M.; Haussinger, D.; Bode, J. G. *J. Immunol.* **2007**, *178*, 2813−2826.

DOI: 10.1021/acs.analchem.6b03214
Anal. Chem. XXXX, XXX, XXX−XXX